Electronic Supplementary Material (ESI) for Physical Chemistry Chemical Physics.

Electronic Supplementary Information for

Large-scale comparison of 3d and 4d transition metal complexes illuminates the reduced effect of exchange on second-row spin-state energetics

Aditya Nandy[1,2,#], Daniel B. K. Chu[1, #], Daniel R. Harper[1,2], Chenru Duan[1,2], Naveen Arunachalam[1], Yael Cytter[1], and Heather J. Kulik[1,*]

[1]*Department of Chemical Engineering, Massachusetts Institute of Technology, Cambridge, MA 02139*

[2]*Department of Chemistry, Massachusetts Institute of Technology, Cambridge, MA 02139*

[#]These authors contributed equally.

Contents

Table S1. Comparison of effects of equilibrium bond length differences from larger basis sets for B3LYP/LACVP* and B3LYP/def2-ZORA-TZVP (i.e., $a_{\mathrm{HF}} = 0.2$) structures of Fe(II) or Ru(II)$(CO)_6$ in HS quintet and LS states. The ratio of the resulting $S(\Delta E_{\text{H-L}})$ between the two basis sets evaluated with that basis set are shown as well along with their individual sensitivities in kcal/mol·HFX. The change in basis set for energetic evaluation is more significant than the change in structure (which is ca. 0.01-0.02 Å). The effect of exchange correlation functional choice (i.e., PBE vs. B3LYP) used in tuning with the LACVP* basis set is also compared on Fe(II)$(CO)_6$ and Ru(II)$(CO)_6$ HS and LS states. Average (avg) metal-ligand bond lengths (M-L dist.) are shown in Å along with the min-max range over all six individual bond lengths unless all bonds are the same in which case the range is indicated as '--'.

Geometric effects				
	B3LYP/LACVP* M-L dist. (Å)		B3LYP/ZORA-def2-TZVP M-L dist. (Å)	
TMC	avg	range	avg	range
LS Ru(II)$(CO)_6$	2.057	--	2.052	--
HS Ru(II)$(CO)_6$	2.479	2.429-2.505	2.457	2.409-2.540
LS Fe(II)$(CO)_6$	1.942	--	1.937	--
HS Fe(II)$(CO)_6$	2.330	2.314-2.361	2.311	2.289-2.322
3*d*:4*d* $S(\Delta E_{\text{H-L}})$ ratio (S in kcal/mol·HFX)	1.8 (-170 / -95)		1.6 (-244 / -156)	
GGA xc effects				
TMC	B3LYP/LACVP*		PBE/LACVP*	
Ru(II)$(CO)_6$ $S(\Delta E_{\text{H-L}})$ kcal/mol·HFX	-95		-81	
Fe(II)$(CO)_6$ $S(\Delta E_{\text{H-L}})$ kcal/mol·HFX	-170		-183	

Table S2. Geometric and electronic criteria adapted from prior work[1] for excluding TMCs from data set with loose geometric cutoffs applied during resubmission indicated in parentheses. The coordination number must be preserved as 6 for all mononuclear octahedral transition metal complexes (i.e., as judged through interatomic distances being within 1.37x the sum of the respective elements' covalent radii). First coordination shell metrics include the mean and maximum (max.) deviation in the angle ($\Delta\theta$) formed with coordinating atoms (C_i or C_j) and the metal from the expected values of 90° or 180° as well as the maximum overall difference between metal-coordinating atom bond lengths over all ligands and specifically in the equatorial (eq.) plane. Ligand distortion metrics include the maximum root mean square deviation (RMSD) of any atom from the starting structure. For ligands that are expected to be linear, additional checks are applied on the deviation of the angle formed by the metal and the first two atoms of the ligand (A, B) from 180°. Tightened checks for homoleptic TMCs are indicated for max(Δd) with a special threshold for singlet states due to our expectation of higher symmetry for these structures.

Geometric criteria			
Coordination number			
6 (6)			
First coordination shell			
mean($\Delta\theta$ (C_i-M-C_j)) 12° (16°)	max($\Delta\theta$(C_i-M-C_j)) 22.5° (27.0°)	max(Δd) 1.00 Å (1.25 Å) homoleptic: 0.4 Å (0.2 Å for singlets)	max(Δd_{eq}) 0.35 Å (0.45 Å)
Ligand distortion metrics			
max(RMSD) 0.30 Å (0.40 Å)		mean($\Delta\theta$(M-A-B)) 20° (30°)	max($\Delta\theta$ (M-A-B)) 28° (40°)
Electronic criteria			
Metal spin		1.0 μ_B	
Deviation of $\langle S^2 \rangle$		1.0 μ_B	

Table S3. Number of 3*d* or 4*d* TMCs eliminated at each sequential filtering step along with how many are retained, and the cumulative total is listed as overall. The filtering steps were: i) convergence (completion, passing loose thresholds upon 5 24 hour job resubmissions), ii) geometry metrics, iii) deviations of $<S^2>$ from the expected value by more than 1 μ_B, and iv) deviations of metal spin of more than 1 μ_B. All calculations were started from converged a_{HF} = 0.20 (i.e., B3LYP results), and then subsequent calculations were attempted at up to a total of six either sequentially increasing (i.e., a_{HF} = 0.25 and 0.30) or decreasing (i.e., a_{HF} = 0.15, 0.10, 0.05, and 0.00) exchange fractions. If the initial B3LYP result did not converge, none of the subsequent calculations were attempted. If one of the subsequent calculations was attempted but failed in either direction, it was also abandoned. This procedure refers only to convergence failures of the geometry optimization or failing loose geometry checks during resubmissions (i.e., step i). All points were checked for steps ii-iv at the end, and failure of one data point to pass the criteria in ii, iii, or iv does not mean that other HF exchange fractions would necessarily be affected.

	3*d* TMCs		4*d* TMCs	
Check Performed	**Retained**	**Eliminated at step**	**Retained**	**Eliminated at step**
Start	26,877	--	19,100	--
Converged	26,326	531	18,743	357
Geometry	23,813	2,513	16,516	2,227
$<S^2>$	22,881	932	16,196	320
Metal spin	21,699	1,182	15,330	866
Overall	**21,699**	**5,178**	**15,330**	**3,770**

Table S4. Summary of computed sensitivities: all *S*(3*d*) or *S*(4*d*) results that were obtained ("results") along with those that were eliminated for having fewer than 4 points or due to the inability to eliminate slope changes between two points. All lines were retained regardless of R^2 values, but any points where LOOCV errors for a point were 5 kcal/mol or higher were eliminated. The cases for which R^2 was below 0.99 are indicated in the $R^2 < 0.99$ subset. The retained results after these filtering steps for both 3*d* and 4*d* TMCs are shown along with the number of matched-ligand pairs that can be generated by identifying metals in the same oxidation/spin states but different principal quantum numbers. These numbers are generally limited by the smaller size of the 4*d* TMC set. Specifics of the filtering procedure: we required that at least four of seven points converged and passed data fidelity checks. We then carried out leave one out cross validation (LOOCV) of the linear fit relationship of a_{HF} with the relevant property (e.g., $\Delta E_{\mathrm{H\text{-}L}}$). Individual points with LOOCV errors greater than 5 kcal/mol were removed along with any points that, upon removal, would increase the R^2 value of the remaining points to above 0.99. If at least four points remained after this first step, the slope was evaluated between each adjacent pair of points, and these slopes were compared for changes in sign as an indication of discontinuous points that had passed the LOOCV check. If the pair of points that changed the sign of the slope included one on the two extrema (i.e., lowest a_{HF} or highest a_{HF} value), they were removed. For any cases that had at least four points after these two filtering steps, a best-fit line and R^2 value was computed on the remaining points. The majority (> 90%) of points after these steps had R^2 values of 0.99 or higher. To ensure fair comparison of properties of 3*d* and 4*d* TMCs, sets formed from matching pairs of ligand fields, oxidation states, and electron configurations across 3*d* and 4*d* metals were obtained. The size of this final data set was primarily limited by the smaller size of the valid 4*d* TMC dataset.

	3d TMCs					**4d TMCs**					**# 3d-4d pairs**
Property	results	< 4 pts.	slope sign	retain	R^2 < 0.99 subset	results	< 4 pts.	slope sign	retain	R^2 < 0.99 subset	
$\Delta E_{\mathrm{H\text{-}L}}$	703	101	2	600	15	399	113	2	284	10	239
$\Delta E_{\mathrm{I\text{-}L}}$	1,072	80	35	957	152	850	180	25	645	91	488
$\Delta E_{\mathrm{H\text{-}I}}$	676	98	4	574	37	361	101	5	255	10	209

Table S5. The ratio of S for $\Delta E_{\text{I-L}}$ to $\Delta E_{\text{H-L}}$ or $\Delta E_{\text{H-I}}$ to $\Delta E_{\text{H-L}}$ for 3*d* and 4*d* TMCs for all 154 TMCs for which all 3 quantities are available, <u>and</u> all sensitivities are negative. The average, standard deviation, minimum, maximum, and range for each ratio is reported.

		3d IS-LS/HS-LS					4d IS-LS/HS-LS				
	Pairs	avg.	std.	min.	max.	range	avg.	std.	min.	max.	range
Cr(II)	11	0.24	0.03	0.20	0.33	0.13	0.36	0.06	0.29	0.48	0.19
Fe(II)	35	0.38	0.07	0.21	0.50	0.29	0.33	0.09	0.12	0.48	0.36
Fe(III)	30	0.42	0.06	0.27	0.51	0.24	0.31	0.11	0.10	0.56	0.47
Mn(II)	36	0.41	0.06	0.28	0.52	0.24	0.38	0.08	0.21	0.72	0.51
Mn(III)	42	0.37	0.05	0.25	0.58	0.33	0.48	0.09	0.31	0.69	0.38
Overall	**154**	**0.38**	**0.07**	**0.20**	**0.58**	**0.39**	**0.38**	**0.11**	**0.10**	**0.72**	**0.62**
		3d HS-IS/HS-LS					4d HS-IS/HS-LS				
		avg.	std.	min.	max.	range	avg.	std.	min.	max.	range
Cr(II)	11	0.76	0.04	0.67	0.83	0.17	0.65	0.07	0.52	0.76	0.23
Fe(II)	35	0.64	0.07	0.52	0.79	0.27	0.67	0.09	0.52	0.86	0.34
Fe(III)	30	0.59	0.07	0.50	0.82	0.32	0.69	0.09	0.53	0.90	0.38
Mn(II)	36	0.59	0.10	0.47	1.09	0.62	0.63	0.08	0.46	0.87	0.42
Mn(III)	42	0.63	0.05	0.45	0.74	0.29	0.53	0.10	0.35	0.81	0.45
Overall	**154**	**0.62**	**0.09**	**0.45**	**1.09**	**0.63**	**0.62**	**0.11**	**0.35**	**0.90**	**0.55**

Table S6. Summary of sensitivities (in kcal/mol·HFX) for pairs of 3*d* and 4*d* TMCs grouped by metal and oxidation state. The total number of 3*d*/4*d* pairs is indicated along with the average, standard deviation, minimum, maximum, and range for the 3*d* or 4*d* TMC subsets. A best-fit line for the relationship between the sensitivities and the associated R^2 value are also shown.

$S(\Delta E_{H\text{-}L})$														
		3d					***4d***					***S(4d) = mS(3d) + C***		
	Pairs	**avg.**	**std.**	**min.**	**max.**	**range**	**avg.**	**std.**	**min.**	**max.**	**range**	**m**	**C**	$\mathbf{R^2}$
Cr(II)	16	-72.2	22.4	-120.1	-33.4	86.7	-45.2	21.9	-74.6	23.2	97.8	0.55	-5.11	0.32
Mn(III)	51	-73.1	18.1	-134.6	-37.2	97.4	-48.5	13.3	-89.3	-27.5	61.9	0.55	-8.24	0.56
Mn(II)	72	-118.9	31.3	-187.1	-62.2	124.8	-76.6	20.9	-137.9	-40.1	97.8	0.53	-13.96	0.63
Fe(III)	36	-80.6	17.0	-120.5	-53.7	66.9	-42.2	19.5	-75.2	45.3	120.5	0.88	28.67	0.59
Fe(II)	64	-110.4	31.6	-175.2	-37.4	137.7	-62.8	16.2	-95.6	-33.5	62.0	0.41	-17.17	0.65
Overall	239	-97.9	33.2	-187.1	-33.4	153.7	-59.6	22.5	-137.9	45.3	183.2	0.55	-5.63	0.67
$S(\Delta E_{H\text{-}I})$														
		3d					***4d***					***S(4d) = mS(3d) + C***		
	Pairs	**avg.**	**std.**	**min.**	**max.**	**range**	**avg.**	**std.**	**min.**	**max.**	**range**	**m**	**C**	$\mathbf{R^2}$
Cr(II)	12	-55.9	13.7	-77.0	-21.5	55.5	-26.7	18.8	-41.4	32.6	74.0	1.13	36.71	0.68
Mn(III)	84	-52.4	15.8	-99.4	-24.2	75.2	-28.7	12.5	-71.1	-12.3	58.8	0.59	2.16	0.55
Mn(II)	38	-68.1	15.1	-110.1	-41.6	68.5	-51.5	15.7	-97.1	-27.6	69.5	0.55	-14.37	0.27
Fe(III)	31	-46.1	7.6	-64.2	-34.4	29.8	-29.4	8.3	-50.0	-15.5	34.5	0.78	6.28	0.50
Fe(II)	44	-73.6	23.1	-157.6	-39.7	117.9	-44.1	15.2	-97.5	-24.6	72.9	0.54	-4.48	0.67
Overall	209	-59.0	19.4	-157.6	-21.5	136.1	-36.1	16.6	-97.5	32.6	130.1	0.65	2.36	0.58
$S(\Delta E_{I\text{-}L})$														
		3d					***4d***					***S(4d) = mS(3d) + C***		
	Pairs	**avg.**	**std.**	**min.**	**max.**	**range**	**avg.**	**std.**	**min.**	**max.**	**range**	**m**	**C**	$\mathbf{R^2}$
Cr(III)	46	-25.2	11.9	-59.8	-6.7	53.1	-20.8	7.4	-41.5	-9.1	32.4	0.42	-10.14	0.46
Cr(II)	88	-18.9	11.8	-63.7	13.7	77.4	-15.5	10.1	-38.7	17.3	56.0	0.16	-12.46	0.04
Mn(III)	77	-31.1	13.3	-81.8	-14.7	67.2	-26.1	17.0	-142.9	-13.6	129.3	0.21	-19.56	0.03
Mn(II)	43	-47.7	20.4	-88.0	-18.2	69.8	-25.5	17.0	-85.1	-3.8	81.3	0.53	-0.14	0.40
Fe(III)	80	-43.5	19.8	-140.7	-18.6	122.1	-15.2	12.6	-73.3	49.7	123.0	0.27	-3.24	0.18
Fe(II)	52	-39.7	23.0	-98.4	17.3	115.6	-18.4	13.3	-42.6	29.5	72.1	0.18	-11.21	0.10
Co(III)	55	-29.5	16.4	-115.5	-4.5	111.0	7.1	8.8	-16.8	36.8	53.6	0.06	8.86	0.01
Co(II)	47	-63.3	24.8	-100.0	-13.2	86.7	-25.1	20.9	-51.4	46.4	97.8	0.64	15.13	0.57
Overall	488	-36.3	22.0	-140.7	17.3	158.0	-18.6	16.3	-142.9	49.7	192.6	0.28	-8.46	0.14

Table S7. Outliers where the *S*(4*d*) value exceeds the *S*(3*d*) value, both shown in kcal/mol·HFX. The R^2 value for each sensitivity determination and the difference between the first-row and second-row sensitivity are shown grouped by the type of spin splitting.

4e HS-LS									
3*d*	4*d*	L_1	L_2	symmetry	*S*(3*d*)	R^2	*S*(4*d*)	R^2	*S*(3*d*)-*S*(4*d*)
Fe(II)	Ru(II)	NH_3	H_2O	trans	-37.4	1.00	-38.0	1.00	0.6
Mn(II)	Tc(II)	$NCCH_3$	CO	5+1	-136.7	1.00	-137.9	0.99	1.2
Mn(II)	Tc(II)	$NCCH_3$	$CNCH_3$	trans	-114.5	0.99	-118.4	0.97	4.0
Mn(III)	Tc(III)	F^-	--	homoleptic	-37.2	1.00	-50.6	0.99	13.5
Cr(II)	Mo(II)	F^-	--	homoleptic	-33.4	0.91	-68.6	0.97	35.3
2e HS-IS									
3*d*	4*d*	L_1	L_2	symmetry	*S*(3*d*)	R^2	*S*(4*d*)	R^2	*S*(3*d*)-*S*(4*d*)
Mn(II)	Tc(II)	CO	H_2O	trans	-57.2	0.97	-76.2	0.99	19.0
Mn(II)	Tc(II)	$NCCH_3$	H_2O	trans	-51.7	1.00	-97.1	0.96	45.5
2e IS-LS									
3*d*	4*d*	L_1	L_2	symmetry	*S*(3*d*)	R^2	*S*(4*d*)	R^2	*S*(3*d*)-*S*(4*d*)
Mn(III)	Tc(III)	H_2S	F^-	5+1	-20.2	1.00	-35.7	0.98	15.5
Fe(II)	Ru(II)	NH_3	CN^-	trans	3.9	0.98	-13.0	1.00	16.9
Cr(II)	Mo(II)	NH_3	H_2S	cis	-2.8	1.00	-20.3	1.00	17.5
Cr(II)	Mo(II)	NH_3	$CNCH_3$	cis	-12.7	0.98	-32.9	0.90	20.2
Cr(II)	Mo(II)	NH_3	CO	trans	13.7	1.00	-13.8	1.00	27.5
Cr(II)	Mo(II)	NH_3	--	homoleptic	-6.4	1.00	-34.1	0.83	27.6
Mn(II)	Tc(II)	$NCCH_3$	$CNCH_3$	trans	-49.3	0.97	-85.1	0.93	35.8
Mn(III)	Tc(III)	Cl^-	$NCCH_3$	5+1	-24.7	0.99	-63.3	0.93	38.6
Mn(III)	Tc(III)	Cl^-	PH_3	5+1	-24.4	1.00	-67.3	0.92	42.9
Mn(III)	Tc(III)	Cl^-	$CNCH_3$	5+1	-31.3	0.99	-77.5	0.95	46.2
Fe(II)	Ru(II)	F^-	CN^-	trans	17.3	0.96	-37.6	1.00	54.9
Mn(III)	Tc(III)	Cl^-	$NCCH_3$	trans	-34.6	0.99	-142.9	0.82	108.3

Table S8. Outliers where the *S*(4*d*) or *S*(3*d*) value is positive (both shown in kcal/mol·HFX) for 4-electron $\Delta E_{\text{H-L}}$ and 2-electron $\Delta E_{\text{H-I}}$. The R^2 value for each sensitivity determination and the difference between the first-row and second-row exchange sensitivity are shown grouped by the type of spin splitting.

4e HS-LS									
3*d*	4*d*	L_1	L_2	symmetry	*S*(3*d*)	R^2	*S*(4*d*)	R^2	*S*(3*d*)-*S*(4*d*)
Cr(II)	Mo(II)	NH_3	Cl^-	cis	-34.0	1.00	23.2	1.00	-57.2
Fe(III)	Ru(III)	F^-	--	homoleptic	-56.9	1.00	45.3	1.00	-102.2
2e HS-IS									
3*d*	4*d*	L_1	L_2	symmetry	*S*(3*d*)	R^2	*S*(4*d*)	R^2	*S*(3*d*)-*S*(4*d*)
Cr(II)	Mo(II)	NH_3	Cl^-	cis	-21.5	1.00	32.6	1.00	-54.1

Table S9. Outliers where the *S*(4*d*) or *S*(3*d*) value is positive (both shown in kcal/mol·HFX) for 2-electron $\Delta E_{\text{I-L}}$. The R^2 value for each sensitivity determination and the sensitivity difference are shown. Only the bottom three cases are $S(3d) > 0$, the rest are $S(4d) > 0$.

3*d*	4*d*	L_1	L_2	symmetry	*S*(3*d*)	R^2	*S*(4*d*)	R^2	*S*(3*d*)-*S*(4*d*)
Co(III)	Rh(III)	$NCCH_3$	NH_3	5+1	-21.1	1.00	19.2	0.84	-40.3
Co(III)	Rh(III)	$NCCH_3$	CO	5+1	-37.9	0.93	14.0	0.95	-51.9
Co(III)	Rh(III)	$NCCH_3$	CN^-	5+1	-35.1	1.00	3.1	0.97	-38.2
Co(III)	Rh(III)	$NCCH_3$	H_2O	5+1	-18.3	0.99	7.7	0.91	-26.1
Co(III)	Rh(III)	NH_3	F^-	5+1	-18.1	1.00	3.3	0.97	-21.4
Co(III)	Rh(III)	$CNCH_3$	CN^-	5+1	-36.7	1.00	4.6	0.87	-41.3
Co(III)	Rh(III)	$CNCH_3$	F^-	5+1	-32.4	1.00	5.3	0.99	-37.7
Co(III)	Rh(III)	H_2O	$NCCH_3$	5+1	-13.8	0.99	6.4	0.97	-20.1
Co(III)	Rh(III)	H_2O	NH_3	5+1	-20.1	0.99	8.9	0.96	-28.9
Co(III)	Rh(III)	H_2O	CO	5+1	-7.9	0.97	11.7	0.98	-19.6
Co(III)	Rh(III)	H_2O	CN^-	5+1	-34.1	1.00	6.7	0.99	-40.8
Co(III)	Rh(III)	H_2O	F^-	5+1	-12.2	0.99	6.2	1.00	-18.5
Co(III)	Rh(III)	NH_3	$NCCH_3$	cis	-24.2	1.00	6.6	0.99	-30.8
Co(III)	Rh(III)	$CNCH_3$	$NCCH_3$	cis	-36.5	1.00	11.8	0.96	-48.3
Co(III)	Rh(III)	H_2O	$NCCH_3$	cis	-14.5	0.99	7.5	0.94	-21.9
Co(III)	Rh(III)	H_2O	NH_3	cis	-23.6	1.00	7.4	0.93	-31.0
Co(III)	Rh(III)	H_2S	Cl^-	cis	-115.5	1.00	6.2	1.00	-121.7
Co(III)	Rh(III)	NH_3	CN^-	cis	-33.2	1.00	7.7	0.91	-40.9
Co(III)	Rh(III)	NH_3	F^-	cis	-19.1	0.99	6.1	0.98	-25.2
Co(III)	Rh(III)	H_2O	F^-	cis	-20.5	1.00	4.9	0.99	-25.4
Co(III)	Rh(III)	$NCCH_3$	$CNCH_3$	cis	-27.4	0.99	12.5	0.96	-39.9
Co(III)	Rh(III)	H_2O	$CNCH_3$	cis	-26.2	1.00	8.2	0.90	-34.4
Co(II)	Rh(II)	F^-	--	homoleptic	-59.0	1.00	46.4	1.00	-105.4
Co(III)	Rh(III)	H_2O	--	homoleptic	-4.5	0.92	5.9	0.89	-10.3
Fe(II)	Ru(II)	CN^-	--	homoleptic	13.5	0.91	17.3	1.00	-3.8
Co(III)	Rh(III)	$NCCH_3$	Cl^-	trans	-19.1	0.89	5.8	1.00	-24.9
Co(III)	Rh(III)	$NCCH_3$	CN^-	trans	-28.2	0.96	9.8	1.00	-38.1
Co(III)	Rh(III)	$NCCH_3$	$CNCH_3$	trans	-26.9	1.00	36.8	0.80	-63.7
Co(III)	Rh(III)	NH_3	Cl^-	trans	-13.1	0.97	9.3	1.00	-22.4
Co(III)	Rh(III)	NH_3	CN^-	trans	-27.0	1.00	15.1	0.99	-42.1
Co(III)	Rh(III)	NH_3	F^-	trans	-9.3	0.99	3.7	0.99	-13.0
Co(III)	Rh(III)	NH_3	H_2O	trans	-26.8	1.00	6.4	0.96	-33.2
Co(III)	Rh(III)	CO	CN^-	trans	-31.9	1.00	5.5	1.00	-37.4
Co(III)	Rh(III)	CO	$CNCH_3$	trans	-22.6	0.93	22.5	0.99	-45.1
Co(III)	Rh(III)	Cl^-	$CNCH_3$	trans	-41.9	0.94	16.2	0.98	-58.1
Co(III)	Rh(III)	Cl^-	PH_3	trans	-38.8	0.98	12.1	0.98	-50.9
Co(III)	Rh(III)	CN^-	NH_3	trans	-37.9	0.96	9.5	0.94	-47.4
Co(III)	Rh(III)	CN^-	F^-	trans	-28.9	0.87	13.4	0.97	-42.3
Co(III)	Rh(III)	CN^-	PH_3	trans	-44.2	1.00	19.5	0.98	-63.6
Co(III)	Rh(III)	H_2S	Cl^-	trans	-25.4	0.96	10.5	1.00	-35.9
Co(III)	Rh(III)	H_2S	CN^-	trans	-32.2	0.99	12.1	1.00	-44.3
Co(III)	Rh(III)	$CNCH_3$	CO	trans	-54.2	1.00	14.4	0.98	-68.7
Co(III)	Rh(III)	$CNCH_3$	CN^-	trans	-37.8	0.99	8.1	0.98	-45.9
Co(III)	Rh(III)	$CNCH_3$	H_2O	trans	-52.9	0.91	9.8	0.90	-62.7
Co(III)	Rh(III)	PH_3	Cl^-	trans	-25.0	0.98	15.9	0.99	-40.9
Co(III)	Rh(III)	H_2O	CO	trans	-9.3	0.96	17.3	0.99	-26.6
Co(III)	Rh(III)	H_2O	$CNCH_3$	trans	-21.4	1.00	3.9	0.89	-25.3
Fe(II)	Ru(II)	CN^-	NH_3	trans	-44.4	0.96	29.5	1.00	-74.0
Fe(II)	Ru(II)	F^-	CO	trans	-15.6	1.00	9.5	1.00	-25.1
Fe(II)	Ru(II)	$CNCH_3$	Cl^-	trans	-44.3	1.00	10.9	0.98	-55.1
Fe(III)	Ru(III)	Cl^-	CN^-	trans	-28.6	1.00	49.7	1.00	-78.3
Fe(II)	Ru(II)	NH_3	CN^-	trans	3.9	0.98	-13.0	1.00	16.9
Cr(II)	Mo(II)	NH_3	CO	trans	13.7	1.00	-13.8	1.00	27.5
Fe(II)	Ru(II)	F^-	CN^-	trans	17.3	0.96	-37.6	1.00	54.9

Table S10. Adiabatic spin-splitting energies, $\Delta E_{\text{H-L}}$, for the 4-electron difference HS-to-LS energies in kcal/mol for 3*d* TMCs containing CO and H_2O ligands with varied a_{HF} values as indicated in the table alongside the computed sensitivity and the R^2 value from a linear fit. Values in italics have been averaged between neighboring points or extrapolated using the linear fit if not between neighboring points. The symmetry and composition of the complex is indicated in the table.

				a_{HF}								
M	CO	H_2O	sym.	0.00	0.05	0.10	0.15	0.20	0.25	0.30	R^2	*S*
Cr(II)	6	0	homoleptic	*2.0*	-5.5	-11.7	*-19.9*	*-28.2*	-36.4	-41.2	1.00	-148.7
Cr(II)	5	1	5+1	-0.8	-7.4	-13.6	-19.4	-24.7	-29.6	-34.0	1.00	-110.5
Cr(II)	4	2	trans	-1.2	-7.8	-14.0	-18.1	-23.4	-28.2	-34.0	1.00	-106.0
Cr(II)	2	4	cis	-14.0	-19.9	-25.4	-30.5	-35.1	-39.2	-42.9	0.99	-96.3
Cr(II)	2	4	trans	-12.0	-18.8	-25.1	-31.0	-36.2	-40.8	-44.7	0.99	-109.5
Cr(II)	1	5	5+1	-22.9	-28.5	-33.6	-38.2	-42.2	-45.8	-48.9	0.99	-86.4
Cr(II)	0	6	homoleptic	-43.7	-45.6	-47.4	-49.1	-50.8	-52.5	-54.1	1.00	-34.4
Mn(III)	6	0	homoleptic	*-16.1*	-19.9	-24.4	-28.5	-32.3	-35.8	-39.1	1.00	-76.6
Mn(III)	5	1	5+1	*-9.2*	-13.5	-18.5	-23.1	-27.4	-31.3	-35.0	1.00	-86.1
Mn(III)	4	2	trans	-6.6	-11.6	-16.3	-20.8	-24.9	-28.8	-32.5	1.00	-86.1
Mn(III)	2	4	cis	-19.8	-24.6	-28.9	-32.9	-36.6	-40.0	-43.2	0.99	-77.7
Mn(III)	2	4	trans	-18.0	-23.1	-27.6	-31.7	-35.5	-39.0	-42.3	0.99	-80.3
Mn(III)	1	5	5+1	-26.2	-30.3	-34.0	-37.4	-40.7	-43.7	-46.6	1.00	-67.6
Mn(III)	0	6	homoleptic	-32.9	-35.3	-38.0	-40.7	-43.3	-45.8	-48.2	1.00	-51.5
Mn(II)	6	0	homoleptic	29.5	19.7	10.5	1.7	-6.6	-14.3	-21.4	1.00	-169.9
Mn(II)	5	1	5+1	20.7	11.1	2.0	-6.5	-14.3	-21.5	-28.1	1.00	-163.0
Mn(II)	4	2	trans	10.8	2.2	-5.9	-13.4	-20.9	-27.5	-34.6	1.00	-150.3
Mn(II)	2	4	cis	-4.0	-12.2	-19.7	-26.7	-33.0	-38.7	-43.7	0.99	-132.4
Mn(II)	2	4	trans	-7.5	-15.3	-22.6	-29.3	-35.4	-40.6	-45.3	0.99	-126.3
Mn(II)	1	5	5+1	-16.1	-23.1	-29.5	-35.4	-40.7	-45.4	-49.5	0.99	-111.4
Mn(II)	0	6	homoleptic	-36.1	-39.7	-43.0	-46.3	-49.1	-51.8	*-54.9*	1.00	-62.7
Fe(III)	6	0	homoleptic	43.4	37.2	29.5	23.7	18.1	12.6	7.3	1.00	-120.5
Fe(III)	5	1	5+1	*33.8*	28.5	22.8	17.4	12.2	7.1	2.0	1.00	-105.7
Fe(III)	4	2	trans	*24.0*	19.5	14.7	10.1	5.6	1.2	-3.2	1.00	-90.5
Fe(III)	2	4	cis	*3.0*	-0.8	-4.9	-8.8	-12.6	-16.4	-20.2	1.00	-77.1
Fe(III)	2	4	trans	1.0	-3.0	-6.8	-10.3	-13.9	-17.4	-20.9	1.00	-72.3
Fe(III)	1	5	5+1	-6.9	-10.4	-13.8	-17.0	-20.3	-23.5	-26.8	1.00	-66.1
Fe(III)	0	6	homoleptic	-15.5	-18.0	-20.6	-23.2	-25.9	-28.7	-31.6	1.00	-53.7
Fe(II)	6	0	homoleptic	64.8	57.1	47.9	38.9	30.3	22.2	14.6	1.00	-170.0
Fe(II)	5	1	5+1	49.2	39.8	31.0	22.6	14.7	7.3	0.5	1.00	-162.5
Fe(II)	4	2	trans	30.1	26.4	18.5	12.8	2.7	-3.3	-8.0	0.99	-135.2
Fe(II)	2	4	cis	17.2	9.5	2.4	-4.3	-10.4	-15.8	-20.7	0.99	-126.5
Fe(II)	2	4	trans	2.9	-3.3	-9.0	-14.3	-19.1	-23.5	-27.4	0.99	-101.3
Fe(II)	1	5	5+1	2.3	-3.7	-9.4	-14.6	-19.4	-23.7	-27.6	0.99	-99.5
Fe(II)	0	6	homoleptic	-15.1	-18.1	-21.1	-23.9	-26.6	-28.6	-31.1	1.00	-53.4
Co(III)	0	6	homoleptic	*5.2*	*4.3*	*3.3*	2.3	1.1	0.9	-0.9	0.92	-19.6

Table S11. Adiabatic spin-splitting energies, $\Delta E_{\text{H-L}}$, for the 4-electron difference HS-to-LS energies in kcal/mol for 4*d* TMCs containing CO and H_2O ligands with varied a_{HF} values as indicated in the table alongside the computed sensitivity and the R^2 value from a linear fit. Values in italics have been averaged between neighboring points or extrapolated using the linear fit if not between neighboring points. The symmetry and composition of the complex is indicated in the table.

				a_{HF}								
M	CO	H_2O	sym.	0.00	0.05	0.10	0.15	0.20	0.25	0.30	R^2	S
Mo(II)	4	2	trans	50.0	47.6	44.8	42.0	39.2	36.5	33.8	1.00	-54.5
Tc(III)	4	2	trans	44.1	40.7	37.3	34.0	*30.9*	27.8	24.9	1.00	-64.0
Tc(III)	2	4	cis	34.7	31.3	28.1	24.9	19.4	16.4	*12.7*	0.99	-74.5
Tc(III)	2	4	trans	41.3	37.5	33.8	30.2	26.8	23.6	20.4	1.00	-69.6
Tc(III)	1	5	5+1	29.3	26.5	23.7	20.9	18.1	15.4	12.7	1.00	-55.4
Tc(III)	0	6	homoleptic	4.4	2.7	1.0	-0.7	-2.5	-4.2	-5.1	1.00	-32.8
Tc(II)	6	0	homoleptic	106.6	100.8	95.1	88.4	83.1	78.0	73.0	1.00	-113.3
Tc(II)	4	2	trans	88.1	82.7	77.4	72.3	68.5	62.6	58.0	1.00	-99.7
Tc(II)	2	4	cis	70.4	65.3	60.2	55.2	50.5	45.8	41.4	1.00	-97.0
Tc(II)	2	4	trans	67.3	62.4	57.7	53.1	48.7	44.5	40.4	1.00	-89.6
Tc(II)	1	5	5+1	52.9	48.5	44.2	40.0	36.0	32.0	28.5	1.00	-81.7
Tc(II)	0	6	homoleptic	11.9	9.7	7.5	5.3	3.2	1.2	-0.8	1.00	-42.4
Ru(III)	6	0	homoleptic	108.2	104.4	100.7	*96.2*	91.8	90.1	86.7	0.99	-72.7
Ru(III)	4	2	trans	*88.2*	*85.5*	*82.7*	79.9	77.1	74.4	71.6	1.00	-55.3
Ru(III)	2	4	cis	*64.5*	*62.1*	*59.6*	57.2	54.7	52.3	49.8	1.00	-48.8
Ru(III)	2	4	trans	*66.0*	*63.7*	61.5	59.2	57.0	54.7	52.4	1.00	-45.5
Ru(III)	1	5	5+1	*52.3*	*50.3*	48.3	46.4	44.4	42.3	40.2	1.00	-40.3
Ru(III)	0	6	homoleptic	*32.6*	*31.5*	30.5	29.6	28.7	27.5	26.3	0.99	-21.2
Ru(II)	6	0	homoleptic	135.3	130.5	125.7	120.9	116.2	111.6	107.0	1.00	-94.5
Ru(II)	4	2	trans	*94.1*	90.1	86.3	82.3	78.2	74.2	70.4	1.00	-79.5
Ru(II)	2	4	cis	81.7	77.8	73.6	69.3	65.1	60.9	56.8	1.00	-83.7
Ru(II)	2	4	trans	61.2	58.0	54.8	51.4	48.0	44.7	41.5	1.00	-65.9
Ru(II)	1	5	5+1	59.2	56.1	52.8	49.4	46.0	42.6	39.3	1.00	-67.0
Ru(II)	0	6	homoleptic	30.0	28.2	26.2	24.3	22.4	20.4	18.5	1.00	-38.4

Table S12. Sensitivities, *S*, in kcal/mol·HFX, for $\Delta E_{\mathrm{H\text{-}L}}$ 4-electron difference adiabatic spin-splitting energies computed among pairs of 3*d* and 4*d* TMCs containing CO and H_2O ligands. The symmetry and composition of the complex is indicated in the table.

M(3*d*)/M(4*d*)	n CO	6-n H_2O	sym.	*S*(3*d*)	*S*(4*d*)
Cr(II)/Mo(II)	4	2	trans	-106.0	-54.5
Mn(III)/Tc(III)	4	2	trans	-86.1	-64.0
Mn(III)/Tc(III)	2	4	cis	-77.7	-74.5
Mn(III)/Tc(III)	2	4	trans	-80.3	-69.6
Mn(III)/Tc(III)	1	5	5+1	-67.6	-55.4
Mn(III)/Tc(III)	0	6	homoleptic	-51.5	-32.8
Mn(II)/Tc(II)	6	0	homoleptic	-169.9	-113.3
Mn(II)/Tc(II)	4	2	trans	-150.3	-99.7
Mn(II)/Tc(II)	2	4	cis	-132.4	-97.0
Mn(II)/Tc(II)	2	4	trans	-126.3	-89.6
Mn(II)/Tc(II)	1	5	5+1	-111.4	-81.7
Mn(II)/Tc(II)	0	6	homoleptic	-62.7	-42.4
Fe(III)/Ru(III)	6	0	homoleptic	-120.5	-72.7
Fe(III)/Ru(III)	4	2	trans	-90.5	-55.3
Fe(III)/Ru(III)	2	4	cis	-77.1	-48.8
Fe(III)/Ru(III)	2	4	trans	-72.3	-45.5
Fe(III)/Ru(III)	1	5	5+1	-66.1	-40.3
Fe(III)/Ru(III)	0	6	homoleptic	-53.7	-21.2
Fe(II)/Ru(II)	6	0	homoleptic	-170.0	-94.5
Fe(II)/Ru(II)	4	2	trans	-135.2	-79.5
Fe(II)/Ru(II)	2	4	cis	-126.5	-83.7
Fe(II)/Ru(II)	2	4	trans	-101.3	-65.9
Fe(II)/Ru(II)	1	5	5+1	-99.5	-67.0
Fe(II)/Ru(II)	0	6	homoleptic	-53.4	-38.4

Table S13. Adiabatic spin-splitting energies, $\Delta E_{\text{H-I}}$, for the 2-electron difference HS-to-IS energies in kcal/mol for 3*d* TMCs containing CO and H_2O ligands with varied a_{HF} values as indicated in the table alongside the computed sensitivity and the R^2 value from a linear fit. Values in italics have been averaged between neighboring points or extrapolated using the linear fit if not between neighboring points. The symmetry and composition of the complex is indicated in the table.

				a_{HF}								
M	CO	H_2O	sym.	0.00	0.05	0.10	0.15	0.20	0.25	0.30	R^2	*S*
Cr(II)	6	0	homoleptic	*21.8*	17.8	13.1	8.8	4.7	0.9	-2.7	1.00	-81.7
Cr(II)	5	1	5+1	18.3	13.7	9.2	5.1	1.1	-2.5	-5.9	1.00	-80.9
Cr(II)	4	2	trans	17.2	12.5	8.1	5.5	1.6	-2.1	-6.8	1.00	-77.0
Cr(II)	2	4	cis	7.5	3.2	-0.8	-4.5	-8.0	-11.1	-14.0	1.00	-71.8
Cr(II)	2	4	trans	3.1	-1.0	-4.7	-8.1	-11.2	-14.0	-16.5	0.99	-65.1
Cr(II)	1	5	5+1	-0.9	-4.6	-8.0	-11.2	-14.1	-16.7	-19.1	0.99	-60.8
Cr(II)	0	6	homoleptic	-15.1	-16.5	-17.8	-19.1	-20.4	-21.7	-22.9	1.00	-26.1
Mn(III)	6	0	homoleptic	17.0	13.5	10.1	7.0	4.1	1.4	-1.2	1.00	-60.6
Mn(III)	5	1	5+1	13.1	9.7	6.6	3.7	0.9	-1.7	-4.2	1.00	-57.5
Mn(III)	4	2	trans	11.5	8.4	5.4	2.6	0.0	-2.6	-4.9	1.00	-54.8
Mn(III)	2	4	cis	0.8	-1.9	-4.4	-6.7	-8.8	-10.8	-12.7	1.00	-44.6
Mn(III)	2	4	trans	3.6	1.1	-1.3	-3.5	-5.7	-7.8	-9.8	1.00	-44.7
Mn(III)	1	5	5+1	-1.3	-3.6	-5.8	-7.8	-9.7	-11.5	-13.3	1.00	-39.7
Mn(III)	0	6	homoleptic	-7.6	-9.1	-10.9	-12.7	-14.5	-16.3	-18.0	1.00	-35.1
Mn(II)	5	1	5+1	-2.0	-7.6	-12.8	-17.6	-22.0	-26.1	-29.8	1.00	-92.6
Mn(II)	4	2	trans	-16.6	-20.8	-24.6	-28.1	-28.3	-31.3	-35.1	0.97	-57.2
Mn(II)	2	4	cis	-20.1	-24.2	-27.8	-31.1	-34.1	-36.8	-39.3	0.99	-63.5
Mn(II)	2	4	trans	-17.1	-21.6	-25.7	-29.4	-32.7	-35.7	-38.4	0.99	-70.7
Mn(II)	1	5	5+1	-21.0	-25.2	-28.9	-32.3	-35.3	-38.0	-40.5	0.99	-64.6
Mn(II)	0	6	homoleptic	-31.4	-33.8	-36.1	-38.3	-40.4	-42.4	-44.3	1.00	-42.9
Fe(III)	6	0	homoleptic	13.3	10.1	7.0	4.0	1.1	-1.7	-4.5	1.00	-59.0
Fe(III)	5	1	5+1	*5.1*	2.4	-0.3	-3.0	-5.6	-8.2	-11.0	1.00	-53.3
Fe(III)	4	2	trans	*-1.8*	*-4.3*	-6.8	-9.1	-13.6	-15.8	-16.0	0.92	-50.1
Fe(III)	2	4	cis	*-6.8*	-9.2	-11.7	-14.0	-16.4	-18.7	-21.1	1.00	-47.4
Fe(III)	2	4	trans	-3.3	-6.2	-8.9	-11.6	-14.1	-16.7	-19.2	1.00	-52.7
Fe(III)	1	5	5+1	-11.1	-13.5	-15.8	-18.0	-20.1	-22.3	-24.5	1.00	-44.4
Fe(III)	0	6	homoleptic	-19.4	-21.1	-22.8	-24.6	-26.3	-28.2	-30.0	1.00	-35.3
Fe(II)	6	0	homoleptic	15.0	11.5	6.6	1.8	-2.7	-6.9	-10.7	1.00	-87.9
Fe(II)	5	1	5+1	13.9	8.2	2.9	-2.1	-6.7	-10.9	-14.7	1.00	-95.4
Fe(II)	4	2	trans	*15.2*	10.4	4.7	1.2	-3.6	-8.1	-14.1	1.00	-94.9
Fe(II)	2	4	cis	*-3.4*	-7.1	-11.8	-16.0	-19.6	-22.8	-25.6	0.99	-73.7
Fe(II)	2	4	trans	-0.9	-5.6	-10.1	-14.3	-18.1	-21.6	-24.7	0.99	-79.6
Fe(II)	1	5	5+1	-3.3	-7.8	-12.1	-15.9	-19.5	-22.6	-25.5	0.99	-73.9
Fe(II)	0	6	homoleptic	-17.8	-19.7	-21.5	-23.1	-24.6	-26.0	-27.2	0.99	-31.3
Co(III)	0	6	homoleptic	*-7.4*	*-8.3*	*-9.1*	-10.0	-10.8	-11.7	-12.5	1.00	-16.8

Table S14. Adiabatic spin-splitting energies, $\Delta E_{\text{H-I}}$, for the 2-electron difference HS-to-IS energies in kcal/mol for 4*d* TMCs containing CO and H_2O ligands with varied a_{HF} values as indicated in the table alongside the computed sensitivity and the R^2 value from a linear fit. Values in italics have been averaged between neighboring points or extrapolated using the linear fit if not between neighboring points. The symmetry and composition of the complex is indicated in the table.

				a_{HF}								
M	CO	H_2O	sym.	0.00	0.05	0.10	0.15	0.20	0.25	0.30	R^2	*S*
Mo(II)	4	2	trans	53.9	52.8	51.1	49.4	47.8	46.1	44.5	1.00	-32.1
Tc(III)	6	0	homoleptic	*49.8*	*48.1*	46.4	44.5	42.8	41.1	39.4	1.00	-34.7
Tc(III)	4	2	trans	48.6	46.4	44.3	42.3	40.4	38.5	36.8	1.00	-39.4
Tc(III)	2	4	cis	35.1	33.1	31.2	29.4	27.6	26.0	24.4	1.00	-35.5
Tc(III)	1	5	5+1	30.2	29.0	27.8	26.6	25.4	24.2	23.0	1.00	-24.0
Tc(III)	0	6	homoleptic	19.1	18.6	18.0	17.4	16.8	16.1	15.4	1.00	-12.3
Tc(II)	4	2	trans	43.2	38.9	34.9	31.1	27.2	22.7	20.9	0.99	-76.2
Tc(II)	2	4	trans	25.7	22.2	18.9	15.8	12.8	10.1	7.5	1.00	-60.8
Ru(III)	4	2	trans	*43.8*	*41.3*	*38.8*	36.3	33.7	31.2	28.8	1.00	-50.0
Ru(III)	2	4	cis	*22.1*	*20.6*	*19.2*	17.7	16.2	14.7	13.3	1.00	-29.3
Ru(III)	2	4	trans	*30.7*	*28.6*	26.6	24.4	22.3	20.3	18.3	1.00	-41.2
Ru(III)	1	5	5+1	*20.4*	*18.8*	17.3	15.6	14.0	12.4	10.9	1.00	-31.6
Ru(III)	0	6	homoleptic	*8.8*	8.0	7.4	6.7	6.0	5.1	4.2	0.99	-15.5
Ru(II)	6	0	homoleptic	*51.5*	*48.7*	*46.0*	43.2	40.3	37.5	34.8	1.00	-55.6
Ru(II)	4	2	trans	*52.2*	48.8	45.3	41.7	38.2	34.9	31.7	1.00	-68.4
Ru(II)	2	4	trans	37.9	35.3	32.5	29.7	26.9	24.2	21.5	1.00	-55.0

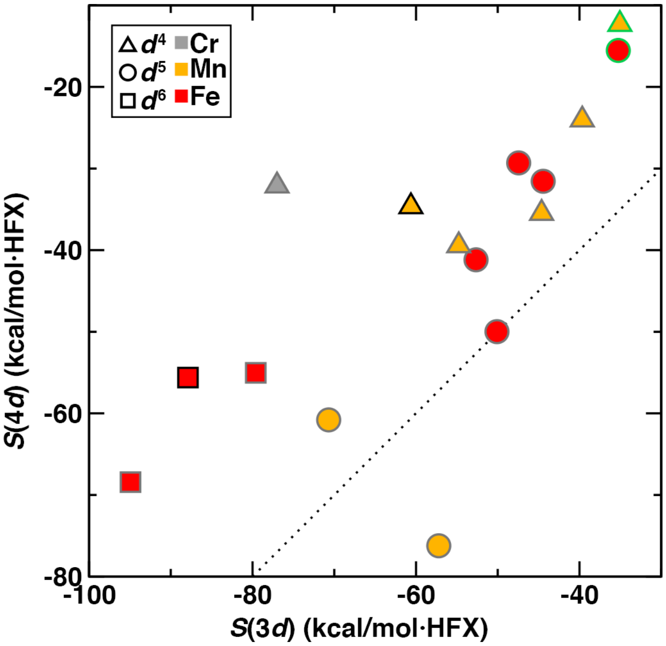

Figure S1. *S*(3d) vs *S*(4d) for $\Delta E_{\text{H-I}}$ (in kcal/mol·HFX) of all TMCs with CO or H_2O ligands in both oxidation states, colored by element (Cr/Mo in gray, Mn/Tc in orange, or Fe/Ru in red) and with symbols corresponding to formal electron configuration (d^4 in triangles, d^5 in circles, and d^6 in squares). All hexa-aqua complexes are outlined in green, all hexa-carbonyl complexes are outlined in black, and the remaining symbols are outlined in dark gray. A dotted parity line is shown for reference.

Table S15. Sensitivities, *S*, in kcal/mol·HFX for $\Delta E_{\mathrm{I\text{-}L}}$ and $\Delta E_{\mathrm{H\text{-}I}}$ 2-electron difference adiabatic spin-splitting energies computed among pairs of 3*d* and 4*d* TMCs containing CO and H_2O ligands. The symmetry and composition of the complex is indicated in the table.

S($\Delta E_{\mathrm{I\text{-}L}}$)					
M(3d)/M(4d)	n CO	6-n H_2O	sym.	*S*(3d)	*S*(4d)
Cr(III)/Mo(III)	4	2	trans	-24.7	-24.7
Cr(III)/Mo(III)	2	4	trans	-22.1	-33.9
Cr(II)/Mo(II)	6	0	homoleptic	-63.7	-12.0
Cr(II)/Mo(II)	4	2	trans	-29.0	-22.4
Cr(II)/Mo(II)	2	4	cis	-26.2	-19.6
Cr(II)/Mo(II)	2	4	trans	-44.6	-29.1
Cr(II)/Mo(II)	1	5	5+1	-25.6	-22.4
Cr(II)/Mo(II)	0	6	homoleptic	-8.3	-9.1
Mn(III)/Tc(III)	4	2	trans	-31.3	-24.7
Mn(III)/Tc(III)	2	4	cis	-33.1	-27.0
Mn(III)/Tc(III)	1	5	5+1	-27.9	-31.3
Mn(III)/Tc(III)	0	6	homoleptic	-16.5	-22.5
Mn(II)/Tc(II)	2	4	trans	-55.6	-28.8
Fe(III)/Ru(III)	2	4	cis	-30.1	-18.5
Fe(III)/Ru(III)	4	2	trans	-19.6	-4.3
Fe(III)/Ru(III)	1	5	5+1	-21.6	-6.5
Fe(III)/Ru(III)	0	6	homoleptic	-18.4	-4.2
Fe(II)/Ru(II)	6	0	homoleptic	-82.1	-37.2
Fe(II)/Ru(II)	4	2	trans	-43.6	-9.7
Fe(II)/Ru(II)	2	4	trans	-21.7	-10.9
Co(III)/Rh(III)	6	0	homoleptic	-48.6	-16.8
Co(III)/Rh(III)	2	4	trans	-9.3	17.3
Co(III)/Rh(III)	1	5	5+1	-7.9	11.7
Co(III)/Rh(III)	0	6	homoleptic	-4.5	5.9
Co(II)/Rh(II)	4	2	trans	-95.4	-50.6
Co(II)/Rh(II)	2	4	trans	-69.9	-36.6
S($\Delta E_{\mathrm{H\text{-}I}}$)					
Cr(II)/Mo(II)	4	2	trans	-77.0	-32.1
Mn(III)/Tc(III)	6	0	homoleptic	-60.6	-34.7
Mn(III)/Tc(III)	4	2	trans	-54.8	-39.4
Mn(III)/Tc(III)	2	4	cis	-44.6	-35.5
Mn(III)/Tc(III)	1	5	5+1	-39.7	-24.0
Mn(III)/Tc(III)	0	6	homoleptic	-35.1	-12.3
Mn(II)/Tc(II)	4	2	trans	-57.2	-76.2
Mn(II)/Tc(II)	2	4	trans	-70.7	-60.8
Fe(III)/Ru(III)	4	2	trans	-50.1	-50.0
Fe(III)/Ru(III)	2	4	cis	-47.4	-29.3
Fe(III)/Ru(III)	2	4	trans	-52.7	-41.2
Fe(III)/Ru(III)	1	5	5+1	-44.4	-31.6
Fe(III)/Ru(III)	0	6	homoleptic	-35.3	-15.5
Fe(II)/Ru(II)	6	0	homoleptic	-87.9	-55.6
Fe(II)/Ru(II)	4	2	trans	-94.9	-68.4
Fe(II)/Ru(II)	2	4	trans	-79.6	-55.0

Table S16. Adiabatic spin-splitting energies, $\Delta E_{\text{I-L}}$, for the 2-electron difference IS-to-LS energies in kcal/mol for 3*d* TMCs containing CO and H_2O ligands with varied a_{HF} values as indicated in the table alongside the computed sensitivity, *S*, and the R^2 value from a linear fit. Values in italics have been averaged or extrapolated using the linear fit if not between neighboring points. The symmetry and composition of the complex is indicated in the table.

				a_{HF}								
M	CO	H_2O	sym.	0.00	0.05	0.10	0.15	0.20	0.25	0.30	R^2	*S*
Cr(III)	2	4	trans	-19.5	-20.9	-22.2	-23.3	-24.3	-25.3	-26.2	0.99	-22.1
Cr(III)	4	2	trans	-18.1	-19.7	-21.1	-22.4	-23.5	-24.6	-25.5	0.99	-24.7
Cr(III)	5	1	5+1	-19.4	-20.8	-22.0	-23.1	-24.2	-25.2	-26.1	0.99	-22.2
Cr(II)	0	6	homoleptic	-28.7	-29.1	-29.5	-30.0	-30.4	-30.8	-31.2	1.00	-8.3
Cr(II)	1	5	5+1	-22.1	-23.9	-25.5	-26.9	-28.1	-29.0	-29.8	0.98	-25.6
Cr(II)	2	4	cis	-21.5	-23.2	-24.6	-26.0	-27.1	-28.1	*-29.4*	0.99	-26.2
Cr(II)	2	4	trans	-15.1	-17.8	*-20.3*	-22.8	-25.0	-26.8	-28.2	0.99	-44.6
Cr(II)	4	2	trans	-18.4	-20.3	-22.1	*-23.5*	-25.0	-26.1	-27.1	0.99	-29.0
Cr(II)	5	1	5+1	*-19.7*	-21.1	-22.9	-24.5	-25.8	-27.0	-28.1	0.99	-27.8
Cr(II)	6	0	homoleptic	-21.9	-23.2	-24.8	-34.6	-36.0	-37.3	-38.5	0.90	-63.7
Mn(III)	0	6	homoleptic	-25.3	-26.2	-27.1	-28.0	-28.8	-29.5	-30.2	1.00	-16.5
Mn(III)	1	5	5+1	-24.9	-26.7	-28.3	-29.7	-31.0	-32.2	-33.3	0.99	-27.9
Mn(III)	2	4	cis	-20.6	-22.7	-24.5	-26.2	-27.8	-29.2	-30.5	0.99	-33.1
Mn(III)	2	4	trans	*-22.6*	-24.2	-26.4	-28.2	-29.8	-31.2	-32.5	0.99	-32.7
Mn(III)	4	2	trans	-18.1	-20.0	-21.8	-23.4	-24.9	-26.3	-27.5	1.00	-31.3
Mn(III)	5	1	5+1	*-21.7*	-23.2	-25.1	-26.7	-28.2	-29.6	-30.8	0.99	-30.4
Mn(III)	6	0	homoleptic	*-32.5*	-33.4	-34.5	-35.6	-36.4	-37.2	-37.9	0.99	-17.8
Mn(II)	0	6	homoleptic	-4.7	-5.9	-6.9	*-7.8*	-8.7	-9.4	*-10.3*	0.99	-18.6
Mn(II)	1	5	5+1	4.9	2.1	-0.6	-3.1	-5.4	-7.4	-9.0	0.99	-46.8
Mn(II)	2	4	cis	16.1	12.0	8.1	4.4	1.1	-1.9	-4.5	0.99	-68.9
Mn(II)	2	4	trans	9.6	6.3	3.1	0.1	-2.7	-4.9	-6.9	0.99	-55.6
Mn(II)	4	2	trans	27.5	23.0	18.7	14.6	7.5	3.9	0.5	0.99	-93.1
Mn(II)	5	1	5+1	22.8	18.7	14.8	11.1	7.7	4.6	1.7	1.00	-70.4
Fe(III)	0	6	homoleptic	4.0	3.1	2.3	1.4	0.4	-0.6	-1.6	1.00	-18.4
Fe(III)	1	5	5+1	4.3	3.1	2.0	1.0	-0.1	-1.2	-2.3	1.00	-21.6
Fe(III)	2	4	cis	10.0	8.3	6.8	5.2	3.7	2.3	0.9	1.00	-30.1
Fe(III)	2	4	trans	4.3	3.2	2.2	1.2	0.3	-0.7	-1.7	1.00	-19.6
Fe(III)	5	1	5+1	29.3	26.1	23.1	20.4	17.8	15.3	13.0	1.00	-54.1
Fe(III)	6	0	homoleptic	30.1	27.1	22.5	19.7	16.9	14.3	11.8	0.99	-61.5
Fe(II)	0	6	homoleptic	2.8	1.6	0.4	-0.8	-2.0	-2.7	-3.9	1.00	-22.2
Fe(II)	1	5	5+1	5.6	4.1	2.7	1.3	0.1	-1.1	-2.1	1.00	-25.7
Fe(II)	2	4	cis	19.1	16.6	14.2	11.7	9.3	7.0	4.9	1.00	-47.8
Fe(II)	2	4	trans	3.8	2.4	1.1	0.0	-1.0	-1.9	-2.7	0.99	-21.7
Fe(II)	4	2	trans	18.1	15.9	13.7	11.6	*9.4*	*7.2*	*5.0*	1.00	-43.6
Fe(II)	5	1	5+1	35.3	31.6	28.1	24.7	21.3	18.2	15.1	1.00	-67.1
Fe(II)	6	0	homoleptic	49.9	45.6	41.3	37.1	33.0	29.1	25.3	1.00	-82.1
Co(III)	0	6	homoleptic	12.8	12.7	12.5	12.3	11.9	*11.7*	*11.4*	0.92	-4.5
Co(III)	1	5	5+1	12.0	11.8	11.5	11.2	10.7	10.2	9.7	0.97	-7.9
Co(III)	2	4	trans	11.8	11.6	11.4	10.9	10.4	9.8	9.1	0.96	-9.3
Co(III)	5	1	5+1	*39.6*	*37.5*	*35.3*	33.1	30.9	28.8	26.7	1.00	-43.1
Co(III)	6	0	homoleptic	47.8	45.1	42.6	40.1	37.7	35.4	33.2	1.00	-48.6
Co(II)	0	6	homoleptic	-13.2	-15.0	-17.0	-18.5	-19.8	-20.7	-21.9	0.98	-28.8
Co(II)	1	5	5+1	-0.7	-5.2	-9.4	-13.5	-16.5	-18.9	-20.8	0.98	-67.8
Co(II)	2	4	trans	1.0	-3.3	-7.4	*-11.0*	-14.6	-17.4	-19.8	0.99	-69.9
Co(II)	4	2	trans	14.9	9.8	4.8	-0.2	-4.9	-9.4	-13.5	1.00	-95.4
Co(II)	5	1	5+1	22.2	16.5	11.0	5.8	0.8	-3.8	-8.2	1.00	-101.5

Table S17. Adiabatic spin-splitting energies, $\Delta E_{\text{I-L}}$, for the 2-electron difference IS-to-LS energies in kcal/mol for 4*d* TMCs containing CO and H_2O ligands with varied a_{HF} values as indicated in the table alongside the computed sensitivity and the R^2 value from a linear fit. Values in italics have been averaged between neighboring points or extrapolated using the linear fit if not between neighboring points. The symmetry and composition of the complex is indicated in the table.

				a_{HF}								
M	CO	H_2O	sym.	0.00	0.05	0.10	0.15	0.20	0.25	0.30	R^2	*S*
Mo(III)	4	2	trans	-3.2	-4.6	-6.0	-7.2	-8.4	-9.6	-10.6	1.00	-24.7
Mo(III)	2	4	trans	-1.9	-4.0	-5.9	-7.8	-9.4	-10.8	-12.0	0.99	-33.9
Mo(III)	1	5	5+1	-7.2	-9.3	-11.2	-12.8	-14.3	-15.7	-16.9	0.99	-32.0
Mo(III)	0	6	homoleptic	*-18.8*	-19.4	-20.1	-20.7	-21.3	*-21.9*	*-22.6*	1.00	-12.6
Mo(II)	6	0	homoleptic	-15.4	-16.1	-16.7	-17.3	*-17.9*	*-18.5*	-19.0	1.00	-12.0
Mo(II)	4	2	trans	-3.9	-5.1	-6.3	-7.5	-8.6	-9.6	-10.6	1.00	-22.4
Mo(II)	2	4	cis	-6.8	-7.9	-8.9	-9.9	-10.8	-11.8	-12.7	1.00	-19.6
Mo(II)	2	4	trans	11.8	10.3	8.8	7.3	5.9	4.5	3.1	1.00	-29.1
Mo(II)	1	5	5+1	1.8	0.6	-0.5	-1.6	-2.7	-3.8	-4.9	1.00	-22.4
Mo(II)	0	6	homoleptic	-17.6	-18.2	-18.7	-19.1	-19.6	-20.0	-20.3	0.99	-9.1
Tc(III)	4	2	trans	-4.5	-5.8	-7.0	-8.3	*-9.5*	-10.7	-11.9	1.00	-24.7
Tc(III)	2	4	cis	-0.4	-1.8	-3.1	-4.5	*-5.8*	*-7.2*	*-8.5*	1.00	-27.0
Tc(III)	1	5	5+1	-0.9	-2.5	-4.1	-5.7	-7.3	-8.8	-10.3	1.00	-31.3
Tc(III)	0	6	homoleptic	-14.7	-15.9	-17.0	-18.2	-19.2	-20.3	*-21.4*	1.00	-22.5
Tc(II)	2	4	trans	41.6	40.2	38.8	37.4	35.9	34.4	33.0	1.00	-28.8
Ru(III)	2	4	cis	42.1	41.2	40.4	39.5	38.5	37.5	36.5	1.00	-18.5
Ru(III)	2	4	trans	*35.5*	*35.3*	*35.1*	34.9	34.7	34.4	34.1	0.90	-4.3
Ru(III)	1	5	5+1	31.2	31.2	31.0	30.8	30.4	29.9	29.3	0.91	-6.5
Ru(III)	0	6	homoleptic	*23.3*	23.1	23.1	22.9	22.7	22.4	22.1	0.96	-4.2
Ru(II)	6	0	homoleptic	*83.4*	*81.5*	*79.6*	77.8	75.9	74.1	72.2	1.00	-37.2
Ru(II)	4	2	trans	41.4	41.3	41.0	40.6	40.0	39.3	38.6	0.96	-9.7
Ru(II)	2	4	trans	23.3	22.8	22.2	21.7	21.1	20.6	20.0	1.00	-10.9
Rh(III)	6	0	homoleptic	*79.6*	78.8	78.0	77.2	76.3	75.5	74.6	1.00	-16.8
Rh(III)	2	4	cis	34.4	35.8	37.0	38.1	39.1	39.8	*40.9*	0.99	21.8
Rh(III)	2	4	trans	25.7	26.8	27.8	28.7	29.5	30.3	30.9	0.99	17.3
Rh(III)	1	5	5+1	29.5	30.4	31.1	31.7	32.2	32.7	33.0	0.98	11.7
Rh(III)	0	6	homoleptic	29.3	29.9	30.3	30.7	30.9	31.0	31.0	0.89	5.9
Rh(II)	4	2	trans	55.0	52.4	49.9	47.4	44.8	42.3	39.8	1.00	-50.6
Rh(II)	2	4	trans	32.3	30.9	29.1	27.3	25.4	23.4	21.5	1.00	-36.6

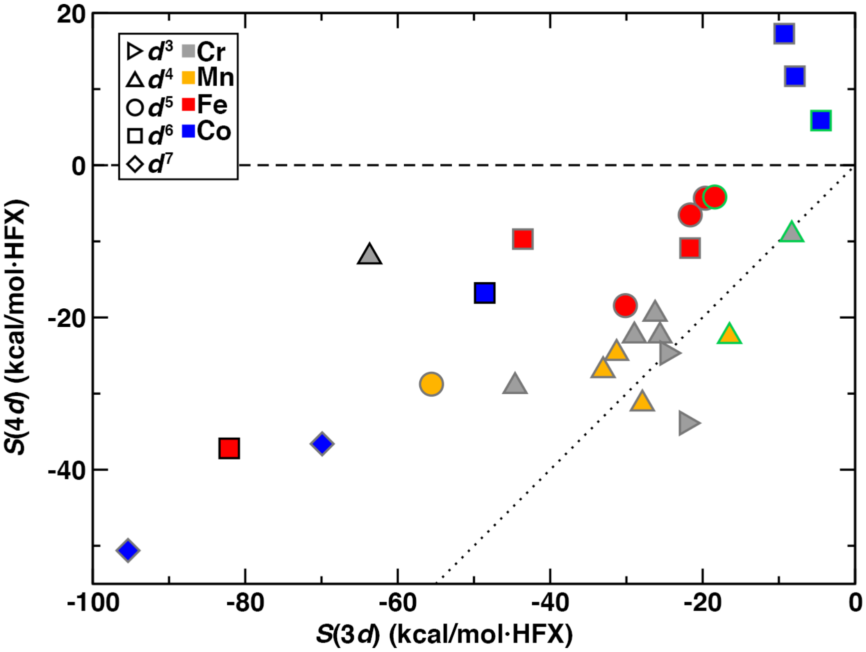

Figure S2. S(3d) vs S(4d) for $\Delta E_{\text{I-L}}$ (in kcal/mol·HFX) of all TMCs with CO or H_2O ligands in both oxidation states, colored by element (Cr/Mo in gray, Mn/Tc in orange, Fe/Ru in red, and Co/Rh in blue) and with symbols corresponding to formal electron configuration (d^3 in right-pointing triangles, d^4 in up-pointing triangles, d^5 in circles, d^6 in squares, and d^7 in diamonds). All hexa-aqua complexes are outlined in green, all hexa-carbonyl complexes are outlined in black, and the remaining symbols are outlined in dark gray. A dotted parity line is shown for reference.

Table S18. Dependence of HS/LS preference based on sign of $\Delta E_{\text{H-L}}$ for all 239 pairs of 3d and 4d complexes for which $\Delta E_{\text{H-L}}$ was evaluated. This analysis is completed for different a_{HF} fractions labeled at the top of the table. The a_{HF} = 0.4 value is extrapolated from the sensitivity. Each preference is grouped by metal and oxidation state and then summarized at the bottom as overall.

	a_{HF} value						a_{HF} value				
3d	0.0	0.1	0.2	0.3	0.4	*4d*	0.0	0.1	0.2	0.3	0.4
Cr(II) LS	0	0	0	0	0	Mo(II) LS	13	13	13	11	10
Cr(II) HS	16	16	16	16	16	Mo(II) HS	3	3	3	5	6
Mn(III) LS	2	0	0	0	0	Tc(III) LS	44	40	34	29	18
Mn(III) HS	49	51	51	51	51	Tc(III) HS	7	11	17	22	33
Mn(II) LS	29	17	4	0	0	Tc(II) LS	72	72	72	71	70
Mn(II) HS	43	55	68	72	72	Tc(II) HS	0	0	0	1	2
Fe(III) LS	28	22	16	10	6	Ru(III) LS	36	36	36	36	36
Fe(III) HS	8	14	20	26	30	Ru(III) HS	0	0	0	0	0
Fe(II) LS	52	39	27	15	5	Ru(II) LS	64	64	64	64	64
Fe(II) HS	12	25	37	49	59	Ru(II) HS	0	0	0	0	0
Overall LS	111	78	47	25	11	Overall LS	229	225	219	211	198
Overall HS	128	161	192	214	228	Overall HS	10	14	20	28	41

Table S19. Dependence of GS preference (HS, LS, or IS) for the 247 pairs for which all compatible spin states have been converged. This corresponds to the 155 pairs of 3*d* and 4*d* complexes for which HS/IS/LS states are all converged in addition to the 92 cases of d^3 Cr(III)/Mo(III) or d^7 Co(II)/Rh(II) pairs for which IS/LS states were converged. The variation is shown with a_{HF} fractions, as labeled at the top of the table. The $a_{\mathrm{HF}} = 0.4$ value is extrapolated from the sensitivity. The overall LS/IS/HS count is shown at the bottom of the table along with the LS/IS count for the d^3/d^7 cases.

	a_{HF} value						a_{HF} value				
3d	0.0	0.1	0.2	0.3	0.4	*4d*	0.0	0.1	0.2	0.3	0.4
Cr(III) LS	2	1	0	0	0	Mo(III) LS	11	10	9	6	5
Cr(III) IS	43	44	45	45	45	Mo(III) IS	34	35	36	39	40
Cr(II) LS	0	0	0	0	0	Mo(II) LS	0	0	0	0	0
Cr(II) IS	9	8	3	1	0	Mo(II) IS	12	12	12	12	12
Cr(II) HS	3	4	9	11	12	Mo(II) HS	0	0	0	0	0
Mn(III) LS	0	0	0	0	0	Tc(III) LS	0	0	0	0	0
Mn(III) IS	22	10	2	2	1	Tc(III) IS	42	42	42	42	42
Mn(III) HS	20	32	40	40	41	Tc(III) HS	0	0	0	0	0
Mn(II) LS	18	12	2	0	0	Tc(II) LS	36	36	36	36	36
Mn(II) IS	0	0	0	0	0	Tc(II) IS	0	0	0	0	0
Mn(II) HS	18	24	34	36	36	Tc(II) HS	0	0	0	0	0
Fe(III) LS	23	18	12	7	5	Ru(III) LS	30	30	30	30	30
Fe(III) IS	0	0	0	0	0	Ru(III) IS	0	0	0	0	0
Fe(III) HS	7	12	18	23	25	Ru(III) HS	0	0	0	0	0
Fe(II) LS	30	21	16	8	3	Ru(II) LS	35	35	35	35	35
Fe(II) IS	1	0	0	0	0	Ru(II) IS	0	0	0	0	0
Fe(II) HS	4	14	19	27	32	Ru(II) HS	0	0	0	0	0
Co(II) LS	38	27	14	10	1	Rh(II) LS	47	47	47	47	47
Co(II) IS	9	20	33	37	46	Rh(II) IS	0	0	0	0	0
d^3/d^7 LS	11	21	33	37	46	d^3/d^7 LS	11	10	9	6	5
d^3/d^7 IS	54	65	78	82	91	d^3/d^7 IS	45	45	45	45	45
Overall LS	111	79	44	25	9	Overall LS	159	158	157	154	153
Overall IS	84	82	83	85	92	Overall IS	88	89	90	93	94
Overall HS	52	86	120	137	146	Overall HS	0	0	0	0	0

Table S20. Dependence of HS/LS preference based on sign of $\Delta E_{\text{H-L}}$ for the 155 pairs of 3*d* and 4*d* complexes for which HS/IS/LS states are all converged with a_{HF} fractions labeled at the top of the table. The a_{HF} = 0.4 value is extrapolated from the sensitivity. This analysis excludes the existence of the IS state and only compares the HS and LS energies. Each preference is grouped by metal and oxidation state and then summarized at the bottom as overall.

	a_{HF} value						a_{HF} value				
3d	0.0	0.1	0.2	0.3	0.4	*4d*	0.0	0.1	0.2	0.3	0.4
Cr(II) LS	0	0	0	0	0	Mo(II) LS	11	11	11	10	9
Cr(II) HS	12	12	12	12	12	Mo(II) HS	1	1	1	2	3
Mn(III) LS	2	0	0	0	0	Tc(III) LS	37	34	29	24	15
Mn(III) HS	40	42	42	42	42	Tc(III) HS	5	8	13	18	27
Mn(II) LS	18	12	2	0	0	Tc(II) LS	36	36	36	36	36
Mn(II) HS	18	24	34	36	36	Tc(II) HS	0	0	0	0	0
Fe(III) LS	23	18	12	7	5	Ru(III) LS	30	30	30	30	30
Fe(III) HS	7	12	18	23	25	Ru(III) HS	0	0	0	0	0
Fe(II) LS	31	21	16	8	3	Ru(II) LS	35	35	35	35	35
Fe(II) HS	4	14	19	27	32	Ru(II) HS	0	0	0	0	0
Overall LS	74	51	30	15	8	Overall LS	149	146	141	135	125
Overall HS	81	104	125	140	147	Overall HS	6	9	14	20	30

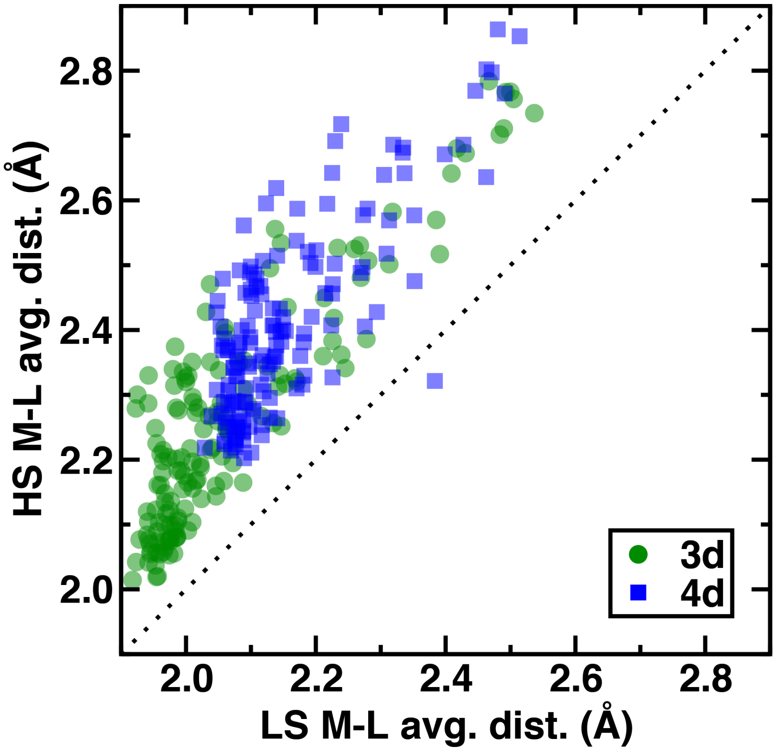

Figure S3. Absolute LS M–L averaged distance (in Å) vs HS M–L averaged distance (in Å) for 155 pairs of equilibrium structures at a_{HF} = 0.2 in the 4-electron LS-to-HS spin state comparison for 3*d* (translucent green circles) and 4*d* (translucent blue squares) TMCs. A black dotted parity line is also shown. All 4*d* TMCs generally have longer bond lengths than 3*d* TMCs due to the larger metal covalent radius.

Table S21. Covalent radii used for 3*d* and 4*d* metals (left) and ligand coordinating elements (right) to obtain relative distances in this work. Recommended covalent radii were obtained from Ref. 2. Where LS and HS covalent radii were provided (e.g., Fe), they were averaged, and where multiple radii based on hybridization (i.e., C) were provided, they were also averaged.

M	r_{cov} (Å)	M	r_{cov} (Å)	L	r_{cov} (Å)	L	r_{cov} (Å)
Cr	1.39	Mo	1.54	C	0.73	He	0.28
Mn	1.50	Tc	1.47	N	0.71	P	1.07
Fe	1.42	Ru	1.46	O	0.66	S	1.05
Co	1.38	Rh	1.42	F	0.57	Cl	1.02

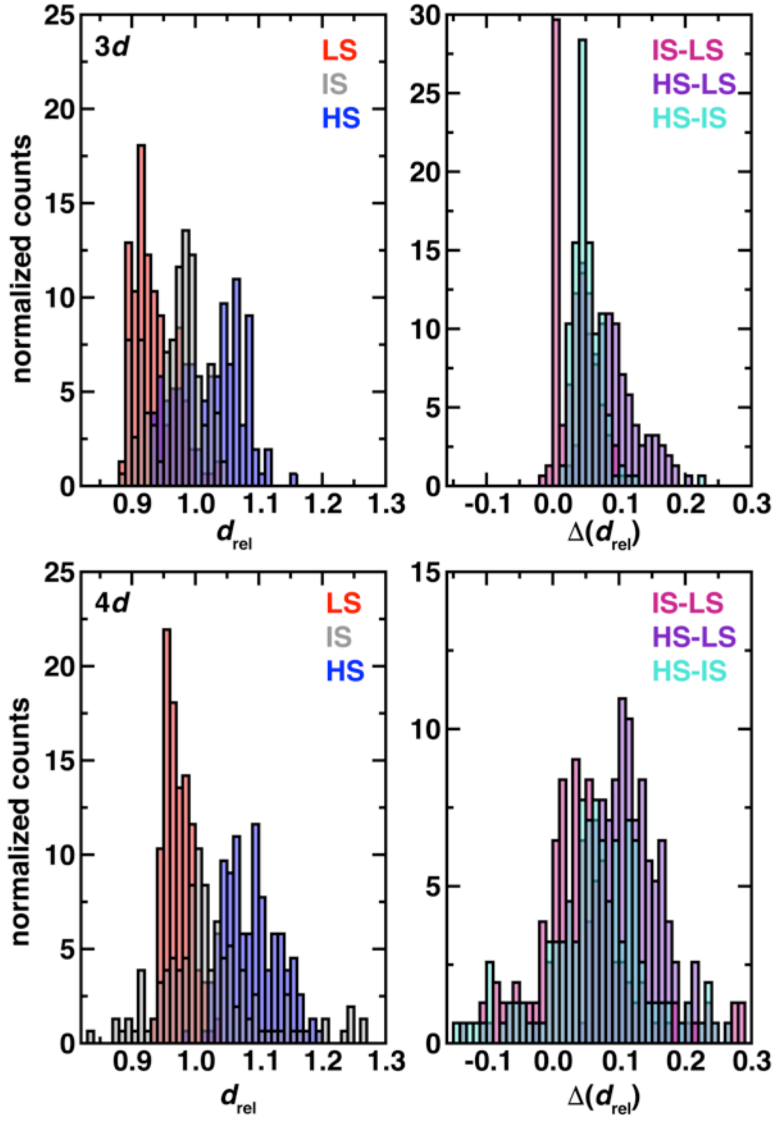

Figure S4. Normalized histograms for 3*d* TMCs (top) and 4*d* TMCs (bottom) with the same x-axis ranges and values for the d_{rel} (left) and difference in d_{rel} (right) plots. The left plots show the averaged (over all 6 metal–ligand bonds) d_{rel} values grouped in translucent histograms by LS (red), IS (gray), and HS (blue) states for 155 (or 247) pairs for which HS, IS, and LS states are all converged (247 is for IS-LS). The right plots show the difference in average d_{rel} values by state of the complexes in translucent normalized histograms: 2-electron IS-LS in magenta, 4-electron HS-LS in purple, and 2-electron HS-IS in cyan.

Table S22. Average, minimum, maximum, and standard deviation (std.) of relative distances for all HS, IS, and LS states as well as the statistics for the HS-LS, IS-LS, and HS-IS differences compared for 155 pairs of 3*d* and 4*d* TMCs for which the LS, IS, and HS states are both defined and successfully converged. The relative distances were computed with respect to the covalent radii of the metal and coordinating atoms and they were then averaged over all equatorial and axial bond lengths. The full distances and covalent radii used are provided in the Supporting Information .zip file.

3*d* TMCs						
	LS	HS	HS-LS	IS	IS-LS	HS-IS
avg	0.93	1.02	0.09	0.97	0.04	0.05
min	0.89	0.93	0.03	0.89	-0.02	0.02
max	1.04	1.15	0.20	1.04	0.11	0.22
std.	0.03	0.05	0.04	0.04	0.03	0.02
4*d* TMCs						
	LS	HS	HS-LS	IS	IS-LS	HS-IS
avg	0.97	1.09	0.12	1.02	0.05	0.06
min	0.94	0.99	-0.03	0.83	-0.14	-0.14
max	1.03	1.20	0.22	1.27	0.29	0.27
std.	0.02	0.04	0.04	0.08	0.08	0.08

Table S23. Average, minimum, maximum, and standard deviation (std.) of relative distances for IS and LS states as well as the statistics for the IS-LS differences compared for 92 pairs of 3*d* and 4*d* TMCs that have d^3 and d^7 electron configurations and therefore only LS and IS states are defined. The relative distances were computed with respect to the covalent radii of the metal and coordinating atoms and they were then averaged over all equatorial and axial bond lengths. The trends in the averages of these LS and IS sets are roughly comparable to those obtained for LS or IS states in the cases where HS states were also valid. The full distances and covalent radii used are provided in the Supporting Information .zip file.

3*d* TMCs			
	LS	IS	IS-LS
avg	0.99	1.03	0.04
min	0.94	0.96	0.00
max	1.06	1.14	0.18
std.	0.02	0.04	0.03
4*d* TMCs			
	LS	IS	IS-LS
avg	1.00	1.04	0.04
min	0.93	0.94	-0.05
max	1.10	1.13	0.08
std.	0.04	0.06	0.03

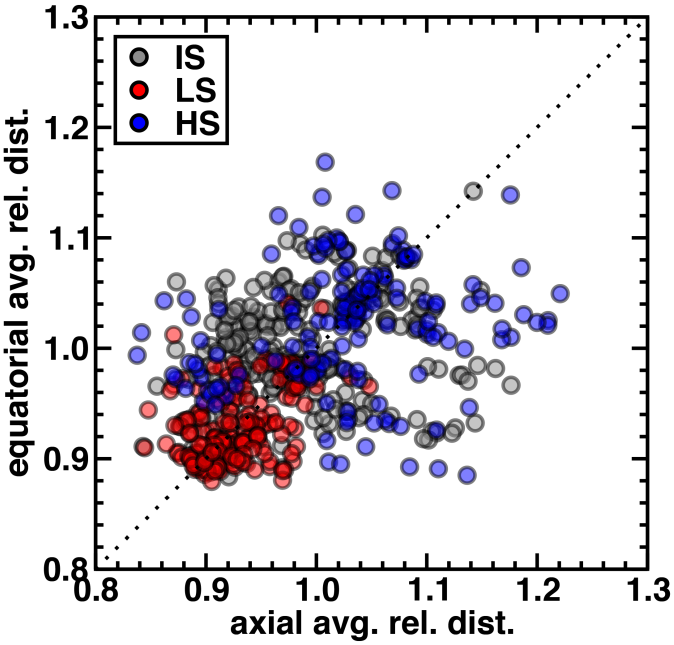

Figure S5. Relative distance averaged over two axial metal–ligand bonds vs. over four equatorial metal–ligand bonds for 3*d* TMCs: 155 pairs of LS (red translucent circles) or HS (blue translucent circles) as well as 247 pairs of IS (gray translucent circles). A parity line is shown in dotted black, and the plot area is square.

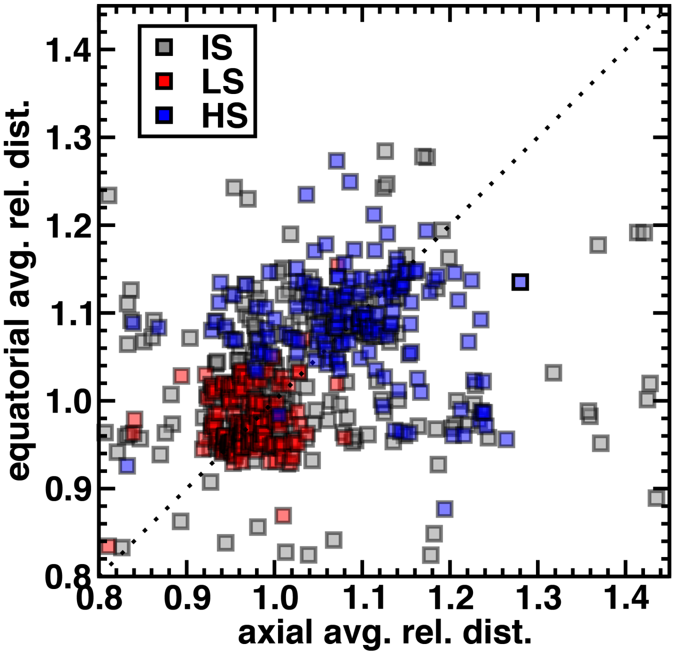

Figure S6. Relative distance averaged over two axial metal–ligand bonds vs. over four equatorial metal–ligand bonds for 4*d* TMCs: 155 pairs of LS (red translucent squares) or HS (blue translucent squares) as well as 247 pairs of IS (gray translucent squares). A parity line is shown in dotted black, and the plot area is square.

Table S24. Best-fit lines (y = mx + b) of the difference in spin state relative bond lengths, Δd_{rel}, vs. sensitivity, $S(\Delta E)$ (in kcal/mol·HFX), for 3*d* TMCs and 4*d* TMCs grouped by relative spin states: 155 cases of 4-electron H-L, 155 cases of 2-electron H-I, and 247 cases of 2-electron I-L. The best-fit line for the overall 3*d* or 4*d* TMC set containing 557 points is also shown. The correlation (R^2) for each line is reported. We also report at the bottom of the table the trendlines obtained for the 3*d* or 4*d* $S(\Delta E_{\mathrm{H\text{-}L}})$ vs. the LS d_{rel} as well as the line obtained by correlating both data sets together.

	m	b	R^2
3*d* H-L	-766.22	-25.518	0.86
3*d* H-I	-657.19	-23.219	0.61
3*d* I-L	-575.25	-21.925	0.55
3*d* overall	-772.62	-18.455	0.81
4*d* H-L	-444.54	-5.305	0.71
4*d* H-I	10.55	-36.818	0.00
4*d* I-L	-13.48	-23.038	0.01
4*d* overall	-126.92	-27.557	0.18
3*d* H-L vs. LS d_{rel}	276.07	-351.44	0.08
4*d* H-L vs. LS d_{rel}	422.87	-468.37	0.16
All H-L vs. LS d_{rel}	532.2	-582.6	0.29

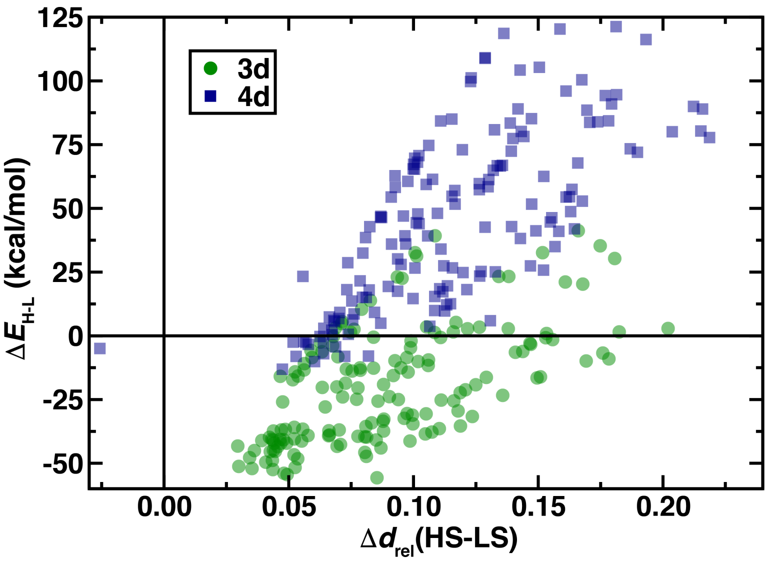

Figure S7. The difference in average relative metal–ligand distance, Δd_{rel}, for the 4-electron HS-LS state comparison vs. $\Delta E_{\mathrm{H\text{-}L}}$ (in kcal/mol) for 155 pairs of HS and LS states at $a_{\mathrm{HF}} = 0.2$ for 3*d* (translucent green circles) and 4*d* (translucent blue squares) TMCs. A zero axis shows when spin state ordering changes or the sign of the relative metal–ligand bond length difference changes.

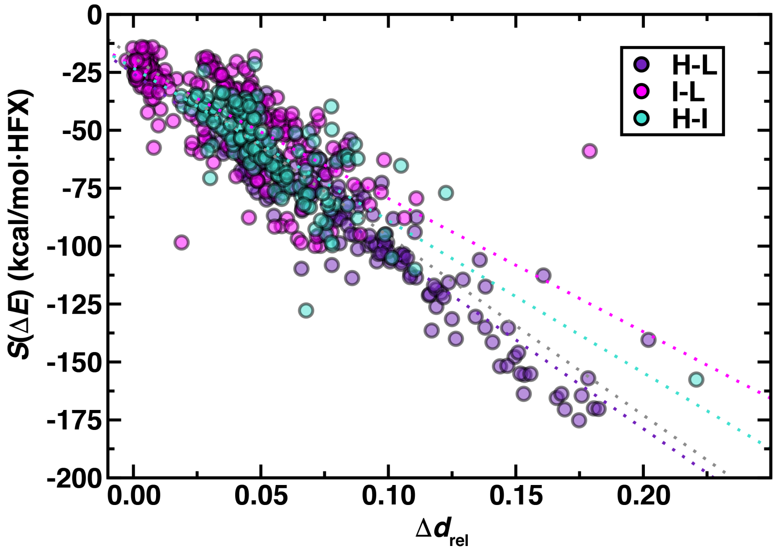

Figure S8. Difference for $3d$ TMCs in average relative distance between relevant spin states, Δd_{rel}, vs the sensitivity of spin state splitting, $S(\Delta E)$, for the same spin states in kcal/mol·HFX grouped by 155 pairs of 4-electron HS-LS (H-L, purple translucent circles), 247 pairs of 2-electron IS-LS (I-L, magenta translucent circles), and 155 pairs of 2-electron HS-IS (H-I, cyan translucent circles). Best-fit lines have been obtained through each spin state definition and shown as dotted solid lines in the same colors. A gray dotted line has been fit through all data.

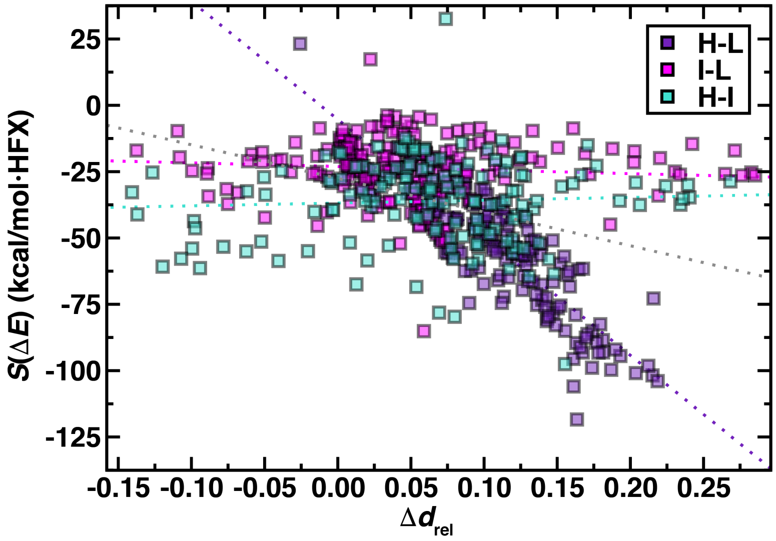

Figure S9. Difference for $4d$ TMCs in average relative distance between relevant spin states, Δd_{rel}, vs the sensitivity of spin state splitting, $S(\Delta E)$, for the same spin states in kcal/mol·HFX grouped by 155 pairs of 4-electron HS-LS (H-L, purple translucent squares), 247 pairs of 2-electron IS-LS (I-L, magenta translucent squares), and 155 pairs of 2-electron HS-IS (H-I, cyan translucent squares). Best-fit lines have been obtained through each spin state definition and shown as dotted solid lines in the same colors. A gray dotted line has been fit through all data.

Table S25. Properties of Fe(II)(He)$_6$ and Ru(II)(He)$_6$ LS and HS complexes: the M–He bond length (in Å) for the LS singlet and HS quintet states, and the relative bond lengths with respect to covalent radii. The sensitivities of the total energies $S(E_{\mathrm{LS}})$ or $S(E_{\mathrm{HS}})$ of the LS and HS states, respectively, are also shown in units of kcal/mol·HFX for both the energies and spin splitting evaluated at the LS geometry (LS vertical) and HS geometry (HS vertical). The adiabatic $S(\Delta E_{\mathrm{H\text{-}L}})$ is also shown evaluated from the equilibrium geometry of both spin states. The $\Delta E_{\mathrm{H\text{-}L}}$ for B3LYP (20% exchange) is shown as well in kcal/mol for each of the three geometries.

		Fe(II)(He)$_6$				
Property	M-He (Å)	d_{rel}	$S(E_{\mathrm{LS}})$	$S(E_{\mathrm{HS}})$	$\Delta E_{\mathrm{H\text{-}L}}$	$S(\Delta E_{\mathrm{H\text{-}L}})$
LS vertical	1.84	1.08	25.64	-21.47	-48.3	-47.12
HS vertical	2.11	1.24	16.30	-21.59	-72.8	-37.89
Adiabatic	--	--	25.64	-21.59	-63.8	-47.25
		Ru(II)(He)$_6$				
Property	M-He (Å)	d_{rel}	$\mathrm{S}(E_{\mathrm{LS}})$	$\mathrm{S}(E_{\mathrm{HS}})$	$\Delta E_{\mathrm{H\text{-}L}}$	$\mathrm{S}(\Delta E_{\mathrm{H\text{-}L}})$
LS vertical	1.93	1.11	-23.12	-63.00	3.4	-39.88
HS vertical	2.35	1.35	-37.96	-66.24	-50.7	-28.28
Adiabatic	--	--	-23.12	-66.24	-31.2	-43.28

Table S26. Properties of Fe(II)(CO)$_6$ and Ru(II)(CO)$_6$ LS and HS complexes: the M–He bond length (in Å) for the LS singlet and HS quintet states, and the relative bond lengths with respect to covalent radii. The sensitivities of the total energies $S(E_{\mathrm{LS}})$ or $S(E_{\mathrm{HS}})$ of the LS and HS states, respectively, are also shown in units of kcal/mol·HFX for both the energies and spin splitting evaluated at the LS geometry (LS vertical) and HS geometry (HS vertical). The adiabatic $S(\Delta E_{\mathrm{H\text{-}L}})$ is also shown evaluated from the equilibrium geometry of both spin states. The $\Delta E_{\mathrm{H\text{-}L}}$ for B3LYP (20% exchange) is shown as well in kcal/mol for each of the three geometries.

		Fe(II)(CO)$_6$				
Property	M-He (Å)	d_{rel}	$S(E_{\mathrm{LS}})$	$S(E_{\mathrm{HS}})$	$\Delta E_{\mathrm{H\text{-}L}}$	$S(\Delta E_{\mathrm{H\text{-}L}})$
LS vertical	1.94	0.90	82.1	-31.9	106.6	-114.1
HS vertical	2.34	1.09	-5.6	-91.6	-19.7	-86.0
Adiabatic	--	--	86.2	-83.8	30.3	-170.0
		Ru(II)(CO)$_6$				
Property	M-He (Å)	d_{rel}	$\mathrm{S}(E_{\mathrm{LS}})$	$\mathrm{S}(E_{\mathrm{HS}})$	$\Delta E_{\mathrm{H\text{-}L}}$	$\mathrm{S}(\Delta E_{\mathrm{H\text{-}L}})$
LS vertical	2.06	0.94	-34.0	-84.9	213.3	-50.9
HS vertical	2.48	1.13	-64.1	-129.1	37.5	-64.9
Adiabatic	--	--	-29.8	-124.3	116.2	-94.5

Table S27. Characteristics of total energy sensitivities for the HS and LS states, $\mathrm{S}(E_{\mathrm{HS}})$ and $S(E_{\mathrm{LS}})$ in kcal/mol·HFX of 3*d* and 4*d* TMCs: minimum, maximum, average, and the number that are positive.

Property	3*d* TMC $S(E_{\mathrm{LS}})$	3*d* TMC $S(E_{\mathrm{HS}})$	4*d* TMC $S(E_{\mathrm{LS}})$	4*d* TMC $S(E_{\mathrm{HS}})$
minimum	-684.3	-776.4	-764.8	-809.4
maximum	148.8	38.5	44.6	-24.0
average	-222.4	-323.1	-290.9	-354.6
# > 0	26	1	2	0

References

1. Nandy, A.; Duan, C.; Janet, J. P.; Gugler, S.; Kulik, H. J., Strategies and Software for Machine Learning Accelerated Discovery in Transition Metal Chemistry. *Industrial & Engineering Chemistry Research* **2018,** *57*, 13973-13986.
2. Cordero, B.; Gómez, V.; Platero-Prats, A. E.; Revés, M.; Echeverría, J.; Cremades, E.; Barragán, F.; Alvarez, S., Covalent Radii Revisited. *Dalton Trans.* **2008**, 2832-2838.